FR9700719

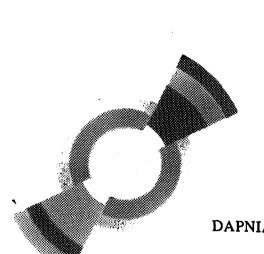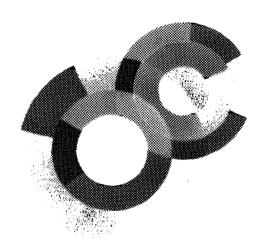# SERVICE DE PHYSIQUE DES PARTICULES

DAPNIA/SPP 96-08   Juin 1996

PROTON STRUCTURE FUNCTIONS IN THE DIPOLE PICTURE OF BFKL DYNAMICS

H. Navelet, R. Peschanski, Ch. Royon, S. Wallon

DAPNIA

29-03
dc

Le DAPNIA (Département d'Astrophysique, de physique des Particules, de physique Nucléaire et de l'Instrumentation Associée) regroupe les activités du Service d'Astrophysique (SAp), du Département de Physique des Particules Elémentaires (DPhPE) et du Département de Physique Nucléaire (DPhN).

Adresse :   DAPNIA, Bâtiment 141
                 CEA Saclay
                 F - 91191 Gif-sur-Yvette Cedex

Proton structure functions in the dipole picture of BFKL dynamics.

H. Navelet[1]
R. Peschanski[1]
Ch. Royon[2]
S. Wallon[1]

1- Service de Physique Théorique, Centre d'Etudes de Saclay

F-91191 Gif-sur-Yvette Cedex, FRANCE

2- DAPNIA - SPP, Centre d'Etudes de Saclay

F-91191 Gif-sur-Yvette Cedex, FRANCE

has been obtained.

is related

Abstract

The $(F_2, F_G, R = F_L/F_2)$ proton structure functions are derived in the QCD dipole picture. Assuming k_T and renormalization-group factorization, we relate deep-inelastic proton scattering to deep-inelastic onium scattering. We get A three-parameter fit of the 1994 H1 data in the low-x, moderate Q^2 range. The ratios F_G/F_2 and R are predicted without further adjustment. The dipole picture of BFKL dynamics is shown to provide a relevant model for quantitatively describing the proton structure functions at HERA. The predictions for F_2 and F_G are compatible with next-to-leading DGLAP analysis, while R is expected to be significantly lower at very small x.

1. Introduction

The purpose of the present paper is to show that the QCD dipole picture [1, 2, 3, 4] provides a pertinent model for describing the proton structure functions at HERA in the low-x and moderate Q^2 range. Indeed the HERA experimental data on the proton structure function and particularly the most recent 1994 published data [5] give a good opportunity to check the validity of different QCD-inspired theoretical models. The QCD dipole model contains the physics of the BFKL Pomeron [6], i.e. the leading $\ln 1/x$ resummation of the perturbative expansion of QCD. In order to apply this model to proton structure function phenomenology, we shall use the k_T-factorization properties [7] in the context of the dipole model. In this scheme we give predictions for the whole set of F_2, F_G and $R = F_L/F_T$ proton structure functions. F_2 is well reproduced with only three parameters and the ratios F_G/F_2 and R are predicted without any further adjustment.

To apply consistently the QCD dipole model to deep-inelastic scattering on a proton, we are led to introduce massive $q\bar{q}$ (onium) configurations inside the proton. On the one hand, we compute the coupling of gluons to the dipole states in an onium (see formulae (9,10)). On the other hand we exhibit factorization constraints on the non-perturbative probabilities of finding an onium into the proton (see formula (19)).

In section **2**, we derive the expression for the onium structure function, including the determination of the gluon-dipole coupling using k_T-factorization. In section **3**, we use once more the k_T-factorization properties to get the predictions for the set of proton structure functions F_T, F_L and F_G. They are obtained as inverse Mellin transforms which can be calculated by the steepest-descent method. In section **4**, we adjust the 3 free parameters of the resulting expressions with the 1994 data on F_2, and give the predictions for F_G and R without further adjustment. The summary of results is in section **5**.

2. Onium structure functions

To get the structure function F_2 we rely on the k_T-dependent factorization properties [7] which are valid at high energy (small x). In a first step, we calculate the deep-inelastic cross-section σ^{onium} of a photon of virtuality Q^2 on an onium state. This onium state can be described by dipole configurations [1]. The photon-onium cross-section reads

$$\sigma^{onium} = \int d^2\underline{r}\,dz\,\Phi^{(0)}(\underline{r}, z)\sigma(x, Q^2; r) \tag{1}$$

where $\Phi^{(0)}(\underline{r}, z)$ is the probability distribution of dipole configurations of transverse coordinate $\underline{r}$.

In the k_T-factorization scheme, one writes

$$Q^2\sigma(x, Q^2; r) = \int^{Q^2} d^2\vec{k} \int_0^1 \frac{dz}{z} \hat{\sigma}(x/z, \vec{k}^2/Q^2)\,F(z, (kr)^2) \tag{2}$$

where $\hat{\sigma}/Q^2$ is the ($\gamma\,g(k) \to q\,\bar{q}$) Born cross section for an off-shell gluon of transverse momentum $\vec{k}$. $F(z, (kr)^2)$ is the unintegrated gluon distribution of an onium state of radius r and contains the physics of the BFKL pomeron. In the x-space, eq.(2) is a convolution . Using the inverse-Mellin transform

$$f(x) = \frac{1}{2i\pi} \int_{c-i\infty}^{c+i\infty} d\omega\; x^{-\omega} f(\omega) \tag{3}$$

yields

$$Q^2\sigma(x,Q^2;r) = \frac{1}{2i\pi}\int d\omega \int d^2\vec{k}\,\hat{\sigma}(\omega,\frac{\vec{k}^2}{Q^2})F(\omega,(kr)^2)r^{-\omega}. \tag{4}$$

A second Mellin transform in the $\vec{k}^2$-space, namely

$$f(\omega,(kr)^2) = \frac{1}{2i\pi}\int_{c-i\infty}^{c+i\infty} d\gamma\, f(\omega,\gamma)(kr)^{2\gamma} \tag{5}$$

yields

$$Q^2\sigma^\gamma(x,Q^2;r) = \int\frac{d\omega}{2i\pi}\int\frac{d\gamma}{2i\pi}\hat{\sigma}(\omega,1-\gamma)F(\omega,\gamma)(Qr)^{2\gamma}r^{-\omega}. \tag{6}$$

Here we have used the Mellin transform of both $\hat{\sigma}$ and F, and taken into account the relation

$$\frac{1}{2i\pi}\int\frac{d\vec{k}^2}{\vec{k}^2}(\vec{k}^2)^{-\gamma-\gamma'+1} = \delta(\gamma'-(1-\gamma)). \tag{7}$$

The unintegrated gluon distribution for an onium of radius r has been derived in the QCD dipole picture. One obtains [1]

$$F(\omega,\gamma) = \frac{1}{\gamma}\frac{v(\gamma)}{\frac{\bar{\alpha}N_c}{\pi}\omega - \chi(\gamma)} \tag{8}$$

where $\chi(\gamma) = 2\Psi(1) - \Psi(\gamma) - \Psi(1-\gamma)$ with $\Psi(\gamma) = \frac{d\ln\Gamma}{d\gamma}$, and $\frac{\bar{\alpha}N_c}{\pi}\chi(\gamma)$ is the well-known BFKL [6] anomalous dimension. $v(\gamma)$ is, up to a factor, the Mellin transform of the gluon-dipole coupling, which expression in the QCD dipole framework we shall now derive.

Using once more the k_T-factorization in extracting a gluon of virtuality l from a dipole of transverse radius r, we find the following expression of v in the momentum space[1, 2]

$$v(rl) = \frac{1}{4\pi}\int_0^{2\pi} d\theta\,(2 - e^{ilr\cos\theta} - e^{-ilr\cos\theta}) \equiv 1 - J_0(lr) \tag{9}$$

and correspondingly

$$v(\gamma) = \int v(lr)(lr)^{-2\gamma-1}d(lr) = \frac{2^{-2\gamma-1}}{\gamma}\frac{\Gamma(1-\gamma)}{\Gamma(1+\gamma)}. \tag{10}$$

A sketchy proof of the determination of $v(lr)$ is obtained by using the eikonal coupling of the off-shell gluon to the dipole of transverse size r. We use the well-known light-cone coordinates as well as the light-cone gauge. When the emitted gluon is soft, the dominant component of its polarization [1] is

$$\epsilon_-^\lambda = \frac{l_-\epsilon^\lambda}{l_+} \tag{11}$$

where ϵ^λ is a two dimensional vector depending on the polarization index λ. Given a quark (antiquark) of transverse coordinate $\underline{x}_0$ ($\underline{x}_1$), the coupling has the form $J_\mu\epsilon^{\mu\lambda} \approx J_+\epsilon_-\lambda$ with the corresponding eikonal current given by

$$J_+ = igT^a(e^{-i\underline{l}.\underline{x}_1} - e^{-i\underline{l}.\underline{x}_0})\frac{2l_+}{l^2}, \tag{12}$$

where $\bar{\alpha} = g^2/(4\pi)$. After averaging over color and polarization, this leads to the cross section

$$\frac{1}{N_c}Tr|J_+\epsilon^\lambda_-|^2 = \frac{1}{N_c}\sum_{\lambda=1,2}g^2Tr(T^aT^a)(e^{-iL\cdot x_1} - e^{-iL\cdot x_0})(e^{iL\cdot x_1} - e^{iL\cdot x_0})4(\frac{L\epsilon^\lambda}{L^2})^2$$

$$= g^2C_F(2 - e^{iL\cdot x_{10}} - e^{-iL\cdot x_{10}})\frac{4}{L^2}. \tag{13}$$

After integrating over the polar angle θ, and with the suitable normalization [7], one gets formula (9). Note that a similar expression is encountered in the elementary dipole-dipole cross section [2].

Since $F(\omega, \gamma)$ (formula (8)) exhibits a pole at $\omega_p = \frac{\bar{\alpha}N_c}{\pi}\chi(\gamma)$, the ω integral yields

$$Q^2\sigma(x, Q^2; r) = \frac{\bar{\alpha}N_c}{\pi}\int\frac{d\gamma}{2i\pi}\hat{\sigma}(\omega = \omega_p, 1-\gamma)\frac{r(\gamma)}{\gamma}(r^2Q^2)^\gamma e^{\frac{\bar{\alpha}N_c}{\pi}\chi(\gamma)\ln(\frac{1}{x})}. \tag{14}$$

Furthermore $\hat{\sigma}(\omega, 1-\gamma)$ is weakly ω-dependent [7], and thus

$$\hat{\sigma}(\omega_p, 1-\gamma) \simeq \hat{\sigma}(0, 1-\gamma) \equiv 4\pi^2\alpha_{e.m.}h(\gamma), \tag{15}$$

factorizing out the electromagnetic coupling.

In order to average over the wave function of the onium state (see formula (1)), one defines

$$< r^2 >^\gamma = \int d^2\underline{r}(r^2)^\gamma dz\ \Phi^{(0)}(\underline{r}, z) = (M^2)^{-\gamma} \tag{16}$$

where M^2 is a *perturbative scale* characterizing the average onium size. This means that M^2 is high enough to use the perturbative dipole-cascade mechanism [1]. The photon-onium structure function then reads

$$F^{onium}(x, Q^2/M^2) = \frac{2\bar{\alpha}N_c}{\pi}\int\frac{d\gamma}{2i\pi}\left(\frac{Q^2}{M^2}\right)^\gamma h(\gamma)\frac{r(\gamma)}{\gamma}e^{\frac{\bar{\alpha}N_c}{\pi}\chi(\gamma)\ln(\frac{1}{x})}$$

$$\equiv \int\frac{d\gamma}{2i\pi}\left(\frac{Q^2}{M^2}\right)^\gamma \sigma(\gamma). \tag{17}$$

where $\sigma(\gamma)$ is the inverse Mellin transform of the onium structure function.

3. Proton structure functions

Let us now deal with deep inelastic scattering on a proton target. Assuming the k_T-factorization properties to be valid for high-energy scattering off a proton target, we substitute in formula (17) $\sigma(\gamma)$ by $\sigma(\gamma)w(\gamma, M^2; Q_0^2)$ where w can be interpreted as the Mellin-transformed probability of finding an onium of transverse mass M^2 in the proton. Q_0^2 is a typically non-perturbative proton scale. Thus,

$$F^{proton}(x, Q^2; Q_0^2) = \frac{2\bar{\alpha}N_c}{\pi}\int\frac{d\gamma}{2i\pi}h(\gamma)\frac{r(\gamma)}{\gamma}\left(\frac{Q^2}{M^2}\right)^\gamma e^{\frac{\bar{\alpha}N_c}{\pi}\chi(\gamma)\ln(\frac{1}{x})}w(\gamma, M^2; Q_0^2). \tag{18}$$

3

As previously mentionned, M^2 is an arbitrary perturbative scale. The overall result has to be independent of the factorization scale, provided it is in the perturbative region. Hence, assuming the renormalization group properties to be valid, the M^2 dependence of w has to match the $(M^2)^{-\gamma}$ dependence of the term $(\frac{Q^2}{M^2})^\gamma$. One then writes

$$w(\gamma, M^2; Q_0^2) = w(\gamma) \left(\frac{M^2}{Q_0^2}\right)^\gamma. \tag{19}$$

The argument leading to formula (19) is similar to the one applied to the one-loop evolution equation in ref. [12].
This yields the final result

$$F^{proton}(x, Q^2; Q_0^2) = \frac{2\bar{\alpha}N_c}{\pi} \int \frac{d\gamma}{2i\pi} h(\gamma) \frac{v(\gamma)}{\gamma} w(\gamma) \left(\frac{Q^2}{Q_0^2}\right)^\gamma e^{\frac{\bar{\alpha}N_c}{\pi}\chi(\gamma)\ln(\frac{1}{x})}. \tag{20}$$

Note that F^{proton} depends on the ratio Q^2/Q_0^2 where Q_0^2 can be interpreted as a characteristic scale of the non perturbative hadron-onium structure function.

Let us use the generic result (20) to derive the prediction for specific proton structure functions in the QCD dipole picture.

$$\begin{pmatrix} F_T \\ F_L \\ F_G \end{pmatrix} = \frac{2\bar{\alpha}N_c}{\pi} \int \frac{d\gamma}{2i\pi} \left(\frac{Q^2}{Q_0^2}\right)^\gamma e^{\frac{\bar{\alpha}N_c}{\pi}\chi(\gamma)\ln(\frac{1}{x})} \begin{pmatrix} h_T \\ h_L \\ 1 \end{pmatrix} \frac{v(\gamma)}{\gamma} w(\gamma) \tag{21}$$

where $F_{T(L)}$ is the structure function corresponding to transverse (longitudinal) photons and F_G the gluon structure function. The coefficient functions

$$\begin{pmatrix} h_T \\ h_L \end{pmatrix} = \frac{\bar{\alpha}}{3\pi\gamma} \frac{(\Gamma(1-\gamma)\Gamma(1+\gamma))^3}{\Gamma(2-2\gamma)\Gamma(2+2\gamma)} \frac{1}{1-\frac{2}{3}\gamma} \begin{pmatrix} (1+\gamma)(1-\frac{\gamma}{2}) \\ \gamma(1-\gamma) \end{pmatrix} \tag{22}$$

are given in ref [7]. Note that the coupling constant $\bar{\alpha}$ in formula (22) will be taken identical to the effective coupling of the BFKL kernel in formula (8). In the following we shall take $\bar{\alpha}$ constant and not running, as in general considered in both BFKL and k_T-factorization schemes.

The integral in γ is performed by the steepest descent method. Assuming that $w(\gamma)$ is smooth and regular near $\gamma = \frac{1}{2}$, we can calculate the structure functions by expansion of the BFKL kernel near this value. The saddle point is at

$$\gamma_c = \frac{1}{2}(1 - a \ln \frac{Q}{Q_0})$$

$$a = \left(\frac{\bar{\alpha}N_c}{\pi} 7\zeta(3) \ln \frac{1}{x}\right)^{-1}. \tag{23}$$

Formulae (23) show that the considered approximation is valid when $a \ln(\frac{Q}{Q_0}) \simeq \ln \frac{Q}{Q_0} / \ln \frac{1}{x} \ll 1$, that is the small x, moderate Q/Q_0 kinematical domain.
We obtain

$$F_2 \equiv F_T + F_L = C a^{1/2} e^{(\omega_P - 1)\ln \frac{1}{x}} \frac{Q}{Q_0} e^{-\frac{a}{2}\ln^2 \frac{Q}{Q_0}}. \tag{24}$$

where

$$\alpha_P - 1 = \frac{4\bar{\alpha} N_C \ln 2}{\pi} .$$ (25)

C, Q_0 and α_P are three unknown parameters which have to be determined by the fit. Once the F_2 fit performed, formula (20) allows one to predict F_G and $R = F_L/F_T$. Moreover R and F_G/F_2 are independent of the overall normalization C, i.e of the non-perturbative $w(\gamma_c)$. One gets

$$\frac{F_G}{F_2} = \frac{1}{h_T + h_L}\bigg|_{\gamma = \gamma_c} \equiv \frac{3\pi\gamma_c}{\bar{\alpha}} \frac{1 - \frac{2}{3}\gamma_c}{1 + \frac{3}{2}\gamma_c - \frac{3}{2}\gamma_c^2} \frac{\Gamma(2 - 2\gamma_c)\Gamma(2 + 2\gamma_c)}{(\Gamma(1 - \gamma_c)\Gamma(1 + \gamma_c))^3}$$ (26)

and

$$R = \frac{h_L}{h_T}(\gamma_c) = \frac{\gamma_c(1 - \gamma_c)}{(1 + \gamma_c)(1 - \frac{\gamma_c}{2})} .$$ (27)

4. Comparison with experiment and predictions

In order to test the accuracy of the F_2 parametrisation obtained in formula (24), a fit using the recently published data from the H1 experiment [5] has been performed. In order to remain in the domain of validity of the QCD dipole model, all the points with $Q^2 \leq 150 \ GeV^2$ were used in the fit (we checked that the result is not strongly dependent on the cut value). The parameters used for the fit are C, Q_0, and α_P. The fit for F_2 is displayed in figure 1. The χ^2 is 101 for 130 points for parameter values:

$$\alpha_P = 1.282$$
$$Q_0 = 0.627 \ GeV.$$
$$C = 0.077$$ (28)

The value of the hard Pomeron intercept α_P is in agreement with values found in other determinations using BFKL dynamics for describing F_2 at HERA [14]. It corresponds to an effective coupling constant $\bar{\alpha} \simeq .11$. As a matter of comparaison, the input value corresponding to the H1 QCD study is .12. As discussed in section 3 of this paper, Q_0 and C are parameters of non-perturbative origin. The value of Q_0, which corresponds to an average transverse size of .3 fermi, is in the range expected for deep inelastic scattering on a proton. C is connected to the non-perturbative input $w(1/2)$.

With only three parameters, the fit of the data is remarkably good in the low Q^2 range. When considering the whole set of H1 data (see fig. 2), deviations from the fit are only observed in the high-Q^2 range ($Q^2 \geq 200 \ GeV^2$), for $x > 10^{-2}$. This is expected since the dipole model does not contains the valence contribution and does not describes the high Q^2 QCD dynamics. By comparison with our previous results [10] based on the H1 and Zeus 1993 data [8], the quality of the present fit confirms the validity of our predictions, while taking into account the extended kinematical domain and the more precise data taken in 1994.

Using formula (26), we get now a precise prediction of the gluon density. The value of $\bar{\alpha}$ we used in formula (26) is the same as for F_2, that is extracted from the fitted value of α_P, by the help of eq.(25). The comparison with the published H1 determination [5] is shown in figure 3. The grey band is the gluon value obtained by the H1 collaboration from their DGLAP next-to-leading order QCD fit for two different values of Q^2. We can

see that our prediction is quite satisfactory without any further adjustment for the H1 values of F_G for $x \leq 5.10^{-2}$ (this parametrisation is not supposed to be valid for higher values of x). We notice that the fit is located in the middle part of the range quoted by the H1 collaboration, while all the gluon density values quoted in the error band are equiprobable [5, 9]. In figure 3, we have also shown the result using only the first-order perturbative expansion of h_T and h_L in Eq.(22). This corresponds to taking

$$\frac{F_G}{F_2} = \frac{3\pi\gamma}{\bar{\alpha}}(1 + \gamma)\Big|_{\gamma=\gamma_c} . \tag{29}$$

The comparison between Eqs. (26) and (29) exhibits the resummation effect of the ln $1/x$ terms on the coefficient functions h_T and h_L. The result of formula (29) is shown as a dotted line in fig.3. The H1 determination clearly favours the resummed result. Our results show in particular that the gluon distribution does not allow to make a distinction between the DGLAP equations, used for the H1 determination, and the BFKL dynamics expressed by the QCD dipole model.

Let us comment the prediction of this model for the value of $R = F_L/F_T$ (formula 27). Let us first notice that this prediction is independent of the non-perturbative normalisation C obtained in the fit of the structure function F_2. The only non-perturbative parameter which enters the R prediction is Q_0. The corresponding curve (full line) is displayed in figure 4. As before, it is useful to compare this prediction with the one-loop one (dotted line), namely $R = \gamma_c$.

The measurement of R might be an opportunity to distinguish between the BFKL and DGLAP mechanisms. One expects the DGLAP predictions for R to be much larger than the limiting value 2/9 obtained in the dipole model. For instance, the theoretical values quoted in [5] are significantly higher than our predictions. It is known that this measurement is very difficult to achieve and the R values are very much correlated to the gluon densities when a QCD fit is performed. However, the fact that a sizeable difference for R is predicted in the same region where F_2 and F_G are well described is an incentive for further studies of R.

5. Summary of results

The main results of our analysis of deep-inelastic scattering can be summarized as follows

i) Using twice the k_T-factorization properties of high-energy hard interactions[7] we were able to give a generic formula for the different structure functions of the proton, and by straightforward extension to any physical target, namely

$$F^{Target}(x.Q^2;Q_0^2) \quad = \frac{2\bar{\alpha}N_c}{\pi} \int \frac{d\gamma}{2i\pi} \left(\frac{Q^2}{Q_0^2}\right)^\gamma h(\gamma)\frac{v(\gamma)}{\gamma}e^{\frac{\bar{\alpha}N_c}{\pi}\chi(\gamma)\ln(\frac{1}{x})}w^{Target}(\gamma). \tag{30}$$

where $h(\gamma)$ is associated[7] to the $(\gamma\, g \to q\, \bar{q})$ Born cross section (see (15)), $v(\gamma)$ is the gluon-dipole coupling function (10) and w^{Target} is the probability of finding an onium in the target.

ii) Using the steepest-descent method, we obtain a 3-parameter expression for F_2 which gives a fair description of all the 94 H1 data with $Q^2 \leq 150 GeV^2$.

iii) Without further adjustment, the model gives definite predictions for F_G and R. One obtains:

$$\frac{F_G}{F_2} = \frac{1}{h_T + h_L}\bigg|_{\gamma = \gamma_c} \; ; \; R = \frac{h_L}{h_T}\bigg|_{\gamma = \gamma_c} \; . \tag{31}$$

where the expression of the saddle-point γ_c is given in formula (23). In particular, the resulting F_G is fully compatible with the determination by H1[5].

iv) The predictions of the QCD dipole model are similar to those obtained through next-to-leading order DGLAP evolution equations. By contrast, R is expected to be significantly lower.

FIGURE CAPTIONS

Figure 1 *3-parameter fit of the H1 proton structure function for* $Q^2 \leq 150\,GeV^2$. The fit is constrained by the 94 data from the H1 experiment [5] (including the point at 2 GeV^2 not shown on the figure for convenience).

Figure 2 *Comparison of the fit with all 94 H1 data.* The validity of the fit extends beyond the domain included in the chi-squared (the highest Q^2 points at 5000 GeV * *2 are not displayed for convenience). We note a discrepancy at high x, and high Q^2, as expected outside the validity of the model.

Figure 3 *Prediction for the gluon density* $F_G(x, Q^2)$. We compare our prediction (full line) (cf. text) with the gluon density obtained by the H1 collaboration [5] (grey band) from their DGLAP next-to-leading order QCD fit. In order to exhibit the resummation effect, we also display the one loop approximation (dotted line), cf. formula (29).

Figure 4 *Prediction for R.* The full line describes our prediction, and is compared to the one-loop approximation (dotted line).

References

[1] A.H.Mueller, *Nucl. Phys.* **B415** (1994) 373.

[2] A.H.Mueller and B.Patel, *Nucl. Phys.* **B425** (1994) 471.

[3] A.H.Mueller, *Nucl. Phys.* **B437** (1995) 107.

[4] N.N.Nikolaev and B.G.Zakharov, *Zeit. für. Phys.* **C49** (1991) 607; *ibid.* **C64** (1994) 651.

[5] H1 coll., S.Aid et al. preprint DESY 96-039, March 1996.

[6] V.S.Fadin, E.A.Kuraev and L.N.Lipatov *Phys. Lett.* **B60** (1975) 50; I.I.Balitsky and L.N.Lipatov, *Sov.J.Nucl.Phys.* **28** (1978) 822.

[7] S.Catani, M.Ciafaloni and Hautmann, *Phys. Lett.* **B242** (1990) 97; *Nucl. Phys.* **B366** (1991) 135; J.C.Collins and R.K.Ellis, *Nucl. Phys.* **B360** (1991) 3; S.Catani and Hautmann, *Phys. Lett.* **B315** (1993) 157; *Nucl. Phys.* **B427** (1994) 475

[8] H1 coll., T.Ahmed et al. *Phys.Lett.* **B348** (1995) 681; ZEUS coll., M.Derrick et al. *Zeit. für. Phys.* **C68** (1995) 569.

[9] J. Feltesse, private communication.

[10] H.Navelet, R.Peschanski and Ch.Royon, *Phys. Lett.* **B366** (1995) 329.

[11] G. Altarelli and G. Parisi, *Nucl. Phys.* **B126** (1977) 298; V.N. Gribov and L.N. Lipatov, *Sov. Journ. Nucl. Phys.* **15** (1972) 138 and 675.

[12] A. De Rújula, S. L. Glashow, H. D. Politzer, S. B. Treiman, F. Wilczek, and A. Zee, *Phys. Rev.* **D10** 1974 1649.

[13] M. Glück, E. Reya and A. Vogt, *Zeit. für Phys.* **C53** (1992) 127; *Phys. Lett.* **B306** (1993) 391.

[14] A.J. Askew, K. Golec-Biernat, J. Kwieciński, A.D. Martin and P.J. Sutton, *Phys. Lett.* **B325** (1994) 212.

F_2

1.5 GeV² 2 GeV² 2.5 GeV² 3.5 GeV² 5 GeV²

F_2

6.5 GeV² 8.5 GeV² 12 GeV² 15 GeV² 20 GeV²

F_2

25 GeV² 35 GeV² 45 GeV² 60 GeV² 90 GeV²

F_2

120 GeV² 150 GeV² 200 GeV² 250 GeV² 350 GeV²

F_2

500 GeV² 650 GeV² 800 GeV² 1200 GeV² 2000 GeV²

10^{-4} 10^{-1} 1 10^{-4} 10^{-1} 1 10^{-4} 10^{-1} 1 10^{-4} 10^{-1} 1 10^{-4} 10^{-1}

x x x x x